HHS Public Access

Author manuscript

Biol Psychiatry. Author manuscript; available in PMC 2018 August 13.

Published in final edited form as:

Biol Psychiatry. 2017 April 15; 81(8): 654–670. doi:10.1016/j.biopsych.2016.09.025.

Adaptive Activation of a Stress Response Pathway Improves Learning and Memory Through Gs and β-Arrestin-1–Regulated Lactate Metabolism

Jun-Hong Dong[#1], **Yi-Jing Wang**[#1], **Min Cui**[#2], **Xiao-Jing Wang**[3], **Wen-Shuai Zheng**[2], **Ming-Liang Ma**[1], **Fan Yang**[4], **Dong-Fang He**[5], **Qiao-Xia Hu**[1], **Dao-Lai Zhang**[5], **Shang-Lei Ning**[6], **Chun-Hua Liu**[2], **Chuan Wang**[7], **Yue Wang**[8], **Xiang-Yao Li**[9], **Fan Yi**[4], **Amy Lin**[10], **Alem W. Kahsai**[10], **Thomas Joseph Cahill III**[10], **Zhe-Yu Chen**[8], **Xiao Yu**[1], and **Jin-Peng Sun**[11]

[1]Key Laboratory Experimental Teratology of the Ministry of Education, Shandong University School of Medicine, China; Department of Biochemistry and Molecular Biology, Shandong University School of Medicine, China.

[2]Physiology, Shandong University School of Medicine, China.

[3]Cell Biology, Shandong University School of Medicine, China.

[4]Key Laboratory Experimental Teratology of the Ministry of Education, Shandong University School of Medicine, China.

[5]Key Laboratory Experimental Teratology of the Ministry of Education, Shandong University School of Medicine, China; Department of Biochemistry and Molecular Biology, Shandong University School of Medicine, China; Physiology, Shandong University School of Medicine, China.

[6]Key Laboratory Experimental Teratology of the Ministry of Education, Shandong University School of Medicine, China; Department of Biochemistry and Molecular Biology, Shandong University School of Medicine, China; Qilu Hospital, Shandong University, Jinan, Shandong, China.

[7]Department of Pharmacology, Hebei Medical University, Shijiazhuang, Hebei, China.

[8]Neurobiology, Shandong University School of Medicine, China.

[9]Zhejiang University, Institute of Neuroscience, China.

[10]Duke University, School of Medicine, Durham, North Carolina.

[11]Key Laboratory Experimental Teratology of the Ministry of Education, Shandong University School of Medicine, China; Department of Biochemistry and Molecular Biology, Shandong University School of Medicine, China; Duke University, School of Medicine, Durham, North Carolina.

Address correspondence to Jin-Peng Sun, Ph.D., Shandong University School of Medicine, 44 Wenhua Xi Road, Jinan, Shandong, 250012, China; sunjinpeng@sdu.edu.cn.

The authors report no biomedical financial interests or potential conflicts of interest.

Supplementary material cited in this article is available online at dx.doi.org/10.1016/j.biopsych.2016.09.025.

[#] These authors contributed equally to this work.

Abstract

BACKGROUND: Stress is a conserved physiological response in mammals. Whereas moderate stress strengthens memory to improve reactions to previously experienced difficult situations, too much stress is harmful.

METHODS: We used specific β-adrenergic agonists, as well as β_2-adrenergic receptor (β2AR) and arrestin knockout models, to study the effects of adaptive β2AR activation on cognitive function using Morris water maze and object recognition experiments. We used molecular and cell biological approaches to elucidate the signaling subnetworks.

RESULTS: We observed that the duration of the adaptive β2AR activation determines its consequences on learning and memory. Short-term formoterol treatment, for 3 to 5 days, improved cognitive function; however, prolonged β2AR activation, for more than 6 days, produced harmful effects. We identified the activation of several signaling networks downstream of β2AR, as well as an essential role for arrestin and lactate metabolism in promoting cognitive ability. Whereas Gs–protein kinase A–cyclic adenosine monophosphate response element binding protein signaling modulated monocarboxylate transporter 1 expression, β-arrestin-1 controlled expression levels of monocarboxylate transporter 4 and lactate dehydrogenase A through the formation of a β-arrestin-1/phospho-mitogen-activated protein kinase/hypoxia-inducible factor-1α ternary complex to upregulate lactate metabolism in astrocyte-derived U251 cells. Conversely, long-term treatment with formoterol led to the desensitization of β2ARs, which was responsible for its decreased beneficial effects.

CONCLUSIONS: Our results not only revealed that β-arrestin-1 regulated lactate metabolism to contribute to β2AR functions in improved memory formation, but also indicated that the appropriate management of one specific stress pathway, such as through the clinical drug formoterol, may exert beneficial effects on cognitive abilities.

Keywords

Adrenergic receptor; Arrestin; G protein; HIF-1α; Memory; Stress

Stress is a conserved biological and psychological response in all mammals, enabling them to react or adapt to challenging environmental changes (1,2). One important process modulated by stress is the ability to memorize and integrate specific information in the stress environment to help individuals effectively respond to similar situations in the future.

Multiple signaling pathways downstream of the stressor regulate brain function in different ways (1–5). The hypothalamus senses the alarm of stress and imparts two main types of reactions: an immediate reaction called “fight or flight behavior,” which is regulated by activation of the adrenergic receptors, and a parallel signal that is regulated by the hypothalamic-pituitary-adrenal axis, which produces glucocorticoids (such as cortisol) to maintain alertness. The exposure to both catecholamine and glucocorticoid stress hormones has been regarded as a double-edged sword (3,4,6). For example, appropriate short-term administration of corticosteroids or adrenergic agonists may be optimal and can produce

risk-appraisal effects in decision making, memory consolidation, and cognitive performance (1,2,7). Conversely, long-term or severely traumatic exposure to corticosteroids impairs the retrieval of long-term spatial memory (8–15). Similarly, long-term administration of β-adrenergic agonists leads to DNA damage and promotes the pathogenesis of Alzheimer's disease (16,17). Therefore, only the optimal activation of a specific stress pathway has the potential to improve learning and memory effectively without unwanted side effects.

The long-acting β_2-adrenergic receptor (β2AR) agonist formoterol was recently reported to relieve nervous system dysfunction in a mouse model of Down syndrome (18). In addition to its neuronal function, β2AR is essential for stress-induced memory consolidation through glycogen breakdown (19–23). Although these studies demonstrated the role of acute β2AR activation in astrocyte glucose metabolism and synaptic activity in a disease model, the adaptive effects of β2AR activation in learning and memory have just begun to be systematically studied (24), and the signaling subnetwork underlying β2AR activity remains elusive. Therefore, we examined the effects of the β2AR agonist formoterol on mouse learning and memory abilities using the Morris water maze and an object recognition (OR) task over various time periods. The changes in the signaling subnetwork after β2AR activation in the hippocampus were then dissected using molecular and cell biological approaches.

METHODS AND MATERIALS

Data Analysis

All data are presented as the mean ± SD of more than three independent experiments. Statistical comparisons were carried out using analysis of variance in GraphPad Prism 5 (GraphPad Software, San Diego, CA) software. Sequence alignments were performed using the T-Coffee multiple sequence alignment program.

All other methods and materials are available in the Supplement.

RESULTS

Duration of Formoterol Administration Determines the Consequence on Learning Ability

We bilaterally injected groups of mice with either the long-acting β2AR agonist formoterol or vehicle before training and then tested the $\beta2AR^{-/-}$ mice and their wild-type littermates in Morris water maze experiments to assess their spatial reference memory. The $\beta2AR^{-/-}$ mice displayed normal cognitive performance and showed no motor impairment (Supplemental Figure S1 and Supplemental Tables S3 and S4). Because the βAR antagonist nadolol does not pass through the blood-brain barrier, we preadministered nadolol (5 mg/kg) before the formoterol treatment to prevent the effects of β2AR activation outside the brain (Figure 1A) (18,25). Compared with vehicle-treated mice, wild-type mice treated with formoterol (2 mg/kg) exhibited significantly shorter escape latencies on days 3, 4, and 5. There were no significant differences from day 6 to day 9, but there were significantly longer escape latencies on days 10 and 11 (Figure 1B and Supplemental Figures S2 and S3). There were no significant differences in body weight or swimming speed between the $\beta2AR^{-/-}$ mice and wild-type mice or between the formoterol-treated and untreated animals,

suggesting that the effects of formoterol on learning ability are not due to a change in mobility (Supplemental Figure S4).

Accordingly, during the hidden platform tests after training, the formoterol-administered wild-type mice displayed statistically significant increases in the number of crosses of the correct platform location compared with vehicle-treated mice on days 3, 4, and 5 (Figure 1C and Supplemental Figure S2); however, they exhibited no differences in crosses on day 7 and showed significant decreases in the number of crosses on day 12 (Figure 1C). The formoterol-treated wild-type mice also performed better in the probe trials on days 3, 4, and 5, but they showed no differences from vehicle-treated mice or even behaved worse on days 7 and 12 (Figure 1D). There were no significant differences between formoterol- and vehicle-treated $\beta 2AR^{-/-}$ mice in all of the above experiments, suggesting that the effect of formoterol in modulating learning ability occurs by the activation of β2AR (Figure 1B–D).

We next tested the effects of the adaptive activation of β2AR on OR (Figure 1E). Compared with vehicle-treated wild-type mice, formoterol-treated wild-type mice spent more time with the novel objects in both short- and long-term OR experiments (Figure 1F, G). However, the formoterol-induced improvement in the discrimination ratio was abolished in the $\beta 2AR^{-/-}$ mice (Figure 1F, G). Taken together, these results suggested that the adaptive activation of β2AR by formoterol for a few days led to improved learning and memory; however, prolonged activation of β2AR showed no beneficial effect.

Transcriptional Profile Analysis Revealed That Activation of the Lactate Metabolism Subnetwork Underlies Adaptive β2AR Signaling to Improve Learning and Memory

We next examined the effect of formoterol on the transcriptional changes of 69 genes in the hippocampus that were previously shown to be associated with memory formation (Figure 2A, B; Supplemental Figure S5 and Supplemental Table S1). Quantitative real-time polymerase chain reaction results revealed that after formoterol administration, the messenger RNA (mRNA) transcript levels of 18 genes were increased, and those of 7 genes were decreased (Supplemental Figure S5). Among these 25 genes, the increased expression of 11 genes and decreased expression of all 7 downregulated genes are dependent on β2AR activation (Figure 2A, B and Supplemental Figure S6). Several genes downstream of the formoterol-induced β2AR activation were shown to be highly enriched in interconnected signaling networks by bioinformatics analysis using KEGG software (www.kegg.jp/kegg/pathway.html) (Figure 2C), including those involved in lactate metabolism and transport (Figure 2D), the glutamate receptor long-term potentiation synaptic signaling pathway (Supplemental Figure S7A), the calcium signaling network (Supplemental Figure S7B), and the neurotrophin signaling pathway (Supplemental Figure S7C).

In the lactate metabolism and transport subnetworks that were transcriptionally activated after formoterol treatment, the genes *Ldha*, *Mct1*, and *Mct4* are key regulators of lactate production and transport and have recently been demonstrated to be required for memory formation by astrocyte-neuron lactate shuttling for supplementing energy (Figure 2D) (26). Therefore, we hypothesized that activation of β2AR might improve learning and memory through the regulation of lactate metabolism. Consistently, formoterol treatment increased lactate levels in the hippocampus and increased protein levels of LDHA, MCT1, and MCT4

(Figure 2E, F). Moreover, costaining for MCT4 and the astrocyte marker glial fibrillary acidic protein revealed significant increases in MCT4 expression in the hippocampus after 3 days of formoterol administration (Figure 2G, H). Notably, the increased lactate levels and LDHA, MCT1, and MCT4 expression by formoterol were abolished in the β2AR$^{-/-}$ mice (Figure 2E, F).

We next injected the inhibitor of glycogen phosphorylation 1,4-dideoxy-1,4-imino-D-arabinitol (DAB) immediately before the OR experiments (26). Treating wild-type mice with formoterol for 3 days significantly increased lactate content in the hippocampus, an effect that was blocked by DAB administration (Figure 2I). Furthermore, the formoterol-induced promotion of memory in the OR experiments was diminished after DAB administration, suggesting that increased lactate metabolism underlies the improved learning and memory after adaptive β2AR activation (Figure 2J, K). The effect of β2AR adaptive activation on lactate metabolism is mainly due to increased gene expression because the application of DAB blocked the lactate increase, but had no significant effect on mRNA levels of *Ldha*, *Mct1*, or *Mct4* (Figure 2L).

Activation of β2AR Promoted Lactate Synthesis and Transportation and the Expression of Key Elements in Lactate Metabolism in a Dose- and Time-Dependent Manner

To further investigate whether upregulation of lactate metabolism and transportation is a general mechanism that occurs after β2AR activation in astrocytes, we tested the effects of formoterol and the endogenous β2AR ligand epinephrine in both primary cultured astrocytes and astrocyte-derived U251 cells. Both epinephrine and formoterol promoted lactate release in primary cultured astrocytes in a dose-dependent manner (Figure 3A, B). Persistent incubation with 10 nmol/L of formoterol increased the total lactate level from 8 hours to 24 hours in cultured astrocyte cells (Figure 3C). Most of the lactate produced by the formoterol-induced synthesis was transported outside the cells (Figure 3D, E).

We next investigated which receptor mediated the effects of formoterol. Formoterol promoted lactate release in the primary astrocytes purified from wild-type and β1AR$^{-/-}$ mice, but not from β2AR$^{-/-}$ mice or β1AR$^{-/-}$/β2AR$^{-/-}$ mice (Figure 3F). Furthermore, the specific β2AR antagonist ICI 118,551 (10 μmol/L) eliminated the formoterol-induced lactate release from the primary astrocytes (Figure 3G). These results demonstrate that the formoterol-induced lactate release was mainly due to activation of the β2AR.

We then evaluated protein and mRNA levels of LDHA, MCT1, and MCT4 in vitro using the astrocyte cell line U251. Formoterol promoted both the mRNA transcription and protein expression of LDHA, MCT1, and MCT4 in both a time-dependent and dose-dependent manner (Figure 3H–M and Supplemental Figure S9). The formoterol-induced increases in LDHA, MCT1, and MCT4 expression were abolished by the β2AR antagonist ICI 118,551 (10 μmol/L) (Figure 3N–O). Therefore, activation of β2AR in astrocytes promoted lactate production and release and the expression of key factors in the lactate metabolic pathway.

The β2AR-Gs-PKA-phosphorylated CREB Signaling Pathway Regulates MCT1 Transcription and Lactate Release

G-protein- and β-arrestin–mediated signaling are the two main pathways underlying β2AR function (17,27–29). Application of the protein kinase A (PKA) inhibitor (E)-N-(2-(4-bromocinna-mylamino)ethyl)isoquinoline-5-sulfonamide dihydrochloride (H89) significantly reduced, but did not eliminate, the formoterol-induced lactate release in U251 cells, demonstrating the contribution of Gs-PKA–mediated β2AR signaling in lactate release (Figure 4A). Further, H89 significantly decreased the protein expression of MCT1, but not of MCT4 or LDHA, after formoterol stimulation (Figure 4B, C).

Phosphorylation of β2AR might result in switching of the receptor to inhibitory G protein (Gi) coupling (20,30). We therefore applied the Gi inhibitor pertussis toxin in U251 cells (31,32). Preincubation of U251 cells with pertussis toxin caused no significant change in lactate release or expression levels of LDHA, MCT1, and MCT4 (Figure 4D–F). Taken together, these results indicate that the Gs-PKA signaling pathway, but not Gi-mediated signaling, contributed to the MCT1 expression and lactate release that are stimulated by formoterol.

The *Mct1* promoter region encompasses two cyclic adenosine monophosphate response element (CRE) enhancers, which are potential binding sites for CRE binding protein (CREB), a transcription factor that is downstream of PKA activation (Figure 4G). Although a mutation of the MCT-M2 CREB binding site showed no significant effect, the MCT-M1/2 double mutant abolished the effects of formoterol (Figure 4H). Application of H89 significantly blocked the formoterol-induced MCT1 transcriptional activity in U251 cells (Figure 4H). Moreover, formoterol promoted CREB phosphorylation at S133 (Figure 4I, J), and this phosphorylation was inhibited by H89 (Figure 4K, L). Therefore, the β2AR-Gs-PKA-phosphorylated CREB-S133 pathway contributes to formoterol-induced MCT1 expression and lactate release.

β-Arrestin-1 Is Required for Formoterol-Induced Increased Lactate Metabolism and Improved Cognitive Ability

After activation of Gs, β2AR is phosphorylated by G protein–coupled receptor kinase and recruits arrestin. Arrestins are important functional regulators of β2AR (28,29,33). We therefore evaluated the functional importance of β-arrestin–mediated signaling using β-arrestin-$1^{-/-}$ and β-arrestin-$2^{-/-}$ mice. Three genes, *Nr1*, *Nmda3a*, and *Adra1a*, showed no significant changes in mRNA levels that were specific to β-arrestin-$2^{-/-}$ mice (Figure 5A, B and Supplemental Figure S10). The increases in mRNA levels of 3 other genes, *Glut2*, *Glut4*, and *CamkIV*, were abolished in both β-arrestin-$1^{-/-}$ and β-arrestin-$2^{-/-}$ mice (Figure 5A, C). In particular, changes in mRNA levels of 10 genes, including *Mct4* and *Ldha*, which are key players in lactate metabolism in astrocytes, were specifically dependent on β-arrestin-1 after formoterol stimulation (Figure 5C, D and Supplemental Figure S11). These results demonstrate that both β-arrestin-1– and β-arrestin-2–dependent signaling underlie the change in transcriptional profile after β2AR activation in the hippocampus, and β-arrestin-1 may play a vital role in the astrocytic lactate metabolism that is required for improved cognitive function after formoterol administration.

We used small interfering RNA to knock down β-arrestin-1 and β-arrestin-2 in U251 cells. The knockdown of β-arrestin-1 impaired the formoterol-induced LDHA and MCT4 expression, whereas the knockdown of β-arrestin-2 had no significant effect on LDHA, MCT1, or MCT4 expression (Figure 5E, F and Supplemental Figure S12). In addition, the knockdown of β-arrestin-1, but not of β-arrestin-2, significantly reduced the formoterol-induced lactate release (Figure 5G and Supplemental Figure S12). Further, β-arrestin-1$^{-/-}$ mice exhibited no significant differences in the cognitive experiments, whereas their wild-type littermates showed improvement in OR after 3 days of daily formoterol administration (Figure 5H, I). Together, these results demonstrate that β-arrestin-1 mediates the improvement of cognitive function and lactate release after adaptive β2AR activation.

Activation of β2AR Regulates MCT4 and LDHA Transcription Through β-Arrestin-1, Which Facilitates the Translocation of Hypoxia-Inducible Factor=1;α

The MCT4 promoter region encompasses three binding sites for the transcription factor hypoxia-inducible factor-1α (HIF-1α) (hypoxia-response elements), and the *Ldha* promoter region contains at least two HIF-1α binding sites (Figure 6A, C). Deletion and mutation analyses indicated that these hypoxia-response elements are important in the formoterol-stimulated *Mct4* and *Ldha* transcriptional activity in U251 cells (Figure 6B, D). Furthermore, the knockdown of β-arrestin-1 almost abolished the transcription of both MCT4 and LDHA by the interaction of the MCT4 and LDHA promoters with HIF-1α.

After formoterol stimulation, HIF-1α accumulated in the nucleus for transcriptional activity in U251 cells (Figure 6E, F). The knockdown of β-arrestin-1, but not β-arrestin-2, significantly reduced HIF-1α levels in the nucleus after formoterol stimulation (Figure 6G, H). Moreover, 3 hours after formoterol stimulation, colocalization was observed between β-arrestin-1–yellow fluorescent protein and HIF-1α in the nucleus (Figure 6I, J). The colocalization of β-arrestin-1–yellow fluorescent protein and hemagglutinin antigen–HIF-1α suggests that β-arrestin-1 may form a complex with HIF-1α after β2AR activation.

Activation of β2AR Leads to Formation of a β-Arrestin-1–Mitogen-Activated Protein Kinase–HIF-1α Ternary Complex and Phosphorylation of HIF-1α at Residues T506 and S515

β-Arrestin-1 has been demonstrated to signal through mitogen-activated protein kinase (ERK) in TGP52 cells (27). In U251 cells, application of the ERK pathway inhibitor U0126 impaired the formoterol-induced nuclear translocation of HIF-1α and blocked the formoterol-stimulated expression of MCT4 and LDHA (Figure 7A–D). Consistently, phospho-ERK, similar to β-arrestin-1, colocalized with hemagglutinin antigen–HIF-1α, which was abolished by β-arrestin-1 small interfering RNA treatment (Figure 7E). Furthermore, after formoterol treatment, the immunoprecipitated hemagglutinin antigen–HIF-1α was bound to both β-arrestin-1 and phospho-ERK, but not to β-arrestin-2 (Figure 7F). Together, these results indicate that β-arrestin-1 mediated HIF-1α activation by the formation of β-arrestin-1/phospho-ERK/HIF-1α ternary complexes.

HIF-1α has several conserved potential ERK phosphorylation sites across different species (Figure 7G). Mutational studies suggest that T506 and S515 are two phosphorylation sites

that are required for HIF-1α nuclear localization after β2AR activation (Figure 7H, I). Together, these results suggest that β-arrestin-1 promotes HIF-1α activity through the formation of a ternary complex of β-arrestin-1/phospho-ERK/HIF-1α and the phosphorylation of HIF-1α at residues T506 and S515.

Prolonged Activation of β2AR Causes Desensitization That Decreases the Beneficial Effect of Formoterol Administration

To investigate how prolonged activation of β2AR decreases its beneficial effects, we examined temporal changes in transcriptional levels of the genes that are enriched in the three β2AR-dependent interconnected signaling networks (Figure 8A–C). Although transcript levels of *Mct1*, *Mct4*, *Glut2*, *Glut4*, *Ldha*, *Nmda3a*, *Adrb3*, and *Adra1a* increased significantly on days 3 and 5, they returned to their basal levels on days 7 and 11 in the hippocampus (Fig. 8A–C). Conversely, although transcript levels of ROL1, glutamate receptor, ionotropic, alpamino-3-hydroxy-5-methyl-4-isoxazolpropionate receptor 4 (AMPA4), mGLUR2, Adra1a, and Adra1d decreased significantly on days 3 and 5 after continuous formoterol administration, they returned to or exceeded normal levels on day 11 after treatment with formoterol. In contrast, control mice showed no significant changes in transcript levels of these selected genes throughout this period (Supplemental Figure S13). These results suggest that the transcriptional profiles are reversed between the short and the prolonged activation of β2AR. We next focused on the network of the lactate metabolism and transport, which has been demonstrated to be driven by activation of ERK and CREB (Figures 3–6). In the hippocampus, both phospho-ERK and phospho-CREB increased on days 3 and 5, followed by significant decreases on days 7 and 11 (Figure 8D–H and Supplemental Figure S14A, B). These results suggest that prolonged formoterol administration impaired β2AR signaling. We therefore examined β2AR protein levels on the plasma membrane using a radioligand binding experiment with 4-[3-[(1,1-dimethylethyl) amino]2-hydroxypropoxy]-1,3-dihydro-2H-benzimidazol-2-one ([^{3}H]-CGP12177) (Figure 8I). We used the specific β1AR antagonist CGP-20712A and the specific β2AR antagonist ICI 118,551 to block β1AR or β2AR binding, respectively. As a result, although β2AR level on the plasma membrane did not show a significant change during the first 5 days of formoterol administration, it decreased significantly from day 7 to day 11 (Figure 8I). Together, these results indicate that prolonged β2AR activation leads to decreased plasma membrane expression of β2AR in the hippocampus, suggesting that a mechanism for β2AR desensitization mediates the impaired β2AR signaling caused by long-term formoterol treatment and decreases the beneficial effect of formoterol on learning and memory.

DISCUSSION

Stressors elevate the reactive ability of humans and animals to adapt to emergent outside changes; these abilities include cognition and memory. Whereas intense or long-term stress has been demonstrated to be harmful (16,17), properly controllable stress may have positive effects. The two main types of hormones found downstream of the stressor are glucocorticoids and catecholamines (2,7,9). The molecular mechanisms of both the acute and adaptive regulation of memory by glucocorticoids have been elucidated (2,10), and studies have shown that emotional stress enhances learning in an acute manner (7). In

parallel to our study, other studies have revealed that hippocampal long-term consolidation of fear-based contextual memory can be mediated by β2AR in astrocytes (24). In the present study, we used the Morris water maze and OR experiments as models to enable the activation of specific βAR signaling using pharmaceutical intervention, at the exclusion of the excessive activation of other endogenous stress signaling pathways. We have demonstrated that in a mouse model, adaptive β2AR activation by the daily administration of 2 mg of formoterol promoted learning and memory from day 3 to day 5 (Figures 1, 8J). However, the persistent activation of β2ARs for more than 7 days was detrimental to cognitive function (Figures 1, 8J). These results confirmed that the appropriate activation of a stress pathway for a few days could be beneficial for memory, and they suggested that persistent activation of β2AR by stress for a period of weeks (more than 1 week) is harmful. Therefore, the proper management of stress signaling such as through β2AR activation by drug administration may improve learning and cognitive abilities.

To unravel the molecular mechanisms that are mediated by adaptive β2AR activation in the modulation of learning and memory, we screened transcriptional profiles of a panel of genes that are functionally important in learning and memory. As a result, we have identified several important signaling subnetworks that are activated downstream of β2AR, including lactate metabolism in astrocyte-neuron circuits and glutamate receptor (both AMPA and metabotropic receptor-based) long-term potentiation signaling (Figure 2A, B, D and Supplemental Figure S6). Recent studies have provided critical evidence that astrocyte-neuron lactate transport is required for long-term memory formation (34). However, the knowledge of how physiological activity or pharmacological intervention, such as stress or treatment with certain drugs, regulates memory through lactate metabolism is just beginning to be appreciated (24). Our cellular and in vivo results suggest that lactate production and transport are important processes that improve learning and memory following adaptive β2AR activation, confirming the significance of the astrocyte-neuron lactate transport energy-supply pathway in cognitive function. Furthermore, we identified that adaptive β2AR activation regulated lactate metabolism by modulating expression of the key factors of both lactate production and transportation, including LDHA, MCT1, and MCT4 (Figures 2, 3). In addition, expression levels of three signaling molecules upstream of the lactate metabolic effectors, GLUT2 to 4, were increased (Figure 2C). Therefore, many steps in lactate metabolism are turned on after adaptive activation of the β2AR-mediated stress pathway.

Two main signaling pathways have been reported to control β2AR activation: G protein–mediated and β-arrestin–mediated pathways (20,27,29,33). Here, we demonstrate that Gs and β-arrestin-1, but not β-arrestin-2, regulate MCT1, MCT4, and LDHA expression. We found that the Gs-PKA pathway regulates MCT1 expression in astrocytes through phosphorylation of CREB, a classic signaling cascade that controls the expression of many proteins relevant to learning and memory (Figures 4, 8J). In parallel to Gs-PKA, we also demonstrated that β-arrestin-1 signaling regulates MCT4 and LDHA expression through formation of a β-arrestin-1/phospho-ERK/HIF-1α ternary complex, which results in the phosphorylation of HIF-1α on pT506/pS515 sites in U251 cells (Figures 7, 8J). Recent studies have shown that β-arrestin-1 and HIF-1α colocalize in a hypoxic environment in breast cancer cells and that β-arrestin-1 facilitates HIF-1α transcriptional activity during prostate cancer cell reprogramming (35,36). However, whether β-arrestin-1–regulated

HIF-1α function mediates normal physiological processes is unknown, and how β-arrestin-1 controls HIF-1α activity remains elusive. Here, we provide the first evidence that G-protein-coupled receptor–regulated HIF-1α activation by β-arrestin-1 mediates ERK activation. Considering that β-arrestin-1–ERK signaling is activated downstream of many receptors, β-arrestin-1–regulated HIF-1α activity may be a general mechanism underlying many receptor functions in various cellular contexts.

More broadly, both the β-arrestin-1– and β-arrestin-2–mediated pathways contribute to transcriptional changes after adaptive β2AR activation (Figure 5A–D). In contrast to genes that are regulated by β-arrestin-1, such as *Mct1*, *Mct4*, and *Ldha*, which are mainly localized in astrocytes, genes regulated by β-arrestin-2, such as *Nr1*, are highly expressed in neurons (Figure 5C, D). Researchers recently discovered that β-arrestin-2–biased signaling downstream of β1AR plays an important role in memory reconsolidation (37). Both their research and our studies unambiguously demonstrate the functional significance of β-arrestin–mediated signaling pathways in cognitive functions. In particular, these results suggest that signaling through a combination of a specific receptor and a specific arrestin subtype may function differently in different brain regions to finely control cognitive functions. The present results, together with recent research on cardiac systems, add to the list of functional divergences between the different arrestin isoforms (38–40).

Taken together, our study demonstrates that the duration of adaptive activation of the β2AR stress signaling pathway determines its consequences on the modulation of learning and memory. Another mechanistic study identified that adaptive activation of β2AR changed the transcriptional profiles of many genes important for learning and memory, including key elements in lactate metabolism and long-term potentiation, which are regulated by both the Gs- and β-arrestin-1–mediated signaling pathways. The current study not only provides a mechanistic insight into how adaptive activation of β2AR modulates learning and memory, but also indicates that the proper control of one specific stress pathway, such as by the administration of formoterol, may exert beneficial effects on human cognitive abilities. The present result may also shed light on the study and use of other drugs, including other ligands for other subtypes of adrenergic receptors, or psychotropic drugs such as methamphetamine and cocaine, in learning and memory.

Supplementary Material

Refer to Web version on PubMed Central for supplementary material.

ACKNOWLEDGMENTS AND DISCLOSURES

This work was supported by the National Key Basic Research Program of China (Grant No. 2013CB967700 to XY; Grant No. 2014CB548200 to X-YL), the National Natural Science Foundation of China (Grant No. 31270857 to XY; Grant Nos. 31271505 and 31470789 to J-PS; Grant No. 81100455 to MC); the Fundamental Research Funds of Shandong University (Grant No. 2014JC029 to XY, Grant No. 2016JC017 to J-PS); the National Science Fund for Distinguished Young Scholars (Grant No. 81525005 to FYi); the Shandong Provincial Natural Science Foundation (Grant No. ZR2014CP007 to D-LZ), the Shandong Natural Science Fund for Distinguished Young Scholars (Grant No. JQ201320 to XY, Grant No. JQ201517 to J-PS), and Innovative Research Team in University (Grant No. IRT13028).

J-PS and XY contributed to the conception and design of the whole research, the analysis and interpretation of the data, and drafting/revising the article. J-HD and Y-JW contributed to the acquisition, analysis of all data; J-HD, Y-

JW, Q-XH, D-FH, MC, C-HL and W-SZ carried out all behavioral studies. YW, J-HD and Z-YC designed and carried out the object cognition experiments. D-LZ purified the primary astrocytes. D-LZ, S-LN, FYa, and CW performed molecular experiments and contributed to the analysis of the data. Y-JW and MC performed the transcriptional studies and immunostaining experiments. AWK, TJC, and FYi contributed to helpful discussion and important experimental designs. All authors approved the final version to be published. J-PS is responsible for the integrity of the work as a whole.

We thank Professor Robert J. Lefkowitz at Duke University and Professor Gang Pei at Tongji University for providing the β-arrestin-1/2 antibodies, β-arrestin-1/2 constructs, and $\beta 2AR^{-/-}$, $Arrb1^{-/-}$, and $Arrb2^{-/-}$ mice.

REFERENCES

1. Kass MD , Rosenthal MC , Pottackal J , McGann JP (2013): Fear learning enhances neural responses to threat-predictive sensory stimuli. Science 342:1389–1392.24337299
2. Chen DY , Bambah-Mukku D , Pollonini G , Alberini CM (2012): Gluco-corticoid receptors recruit the CaMKIIalphaBDNF-CREB pathways to mediate memory consolidation. Nat Neurosci 15:1707–1714.23160045
3. de Kloet ER , Joels M , Holsboer F (2005): Stress and the brain: From adaptation to disease. Nat Rev Neurosci 6:463–475.15891777
4. Barsegyan A , Mackenzie SM , Kurose BD , McGaugh JL , Roozendaal B (2010): Glucocorticoids in the prefrontal cortex enhance memory consolidation and impair working memory by a common neural mechanism. Proc Natl Acad Sci U S A 107:16655–16660.20810923
5. Karst H , Berger S , Erdmann G , Schutz G , Joels M (2010): Metaplasticity of amygdalar responses to the stress hormone corticosterone. Proc Natl Acad Sci U S A 107:14449–14454.20663957
6. Liu X , Betzenhauser MJ , Reiken S , Meli AC , Xie W , Chen BX , et al. (2012): Role of leaky neuronal ryanodine receptors in stress-induced cognitive dysfunction. Cell 150:1055–1067.22939628
7. Hu H , Real E , Takamiya K , Kang MG , Ledoux J , Huganir RL , Malinow R (2007): Emotion enhances learning via norepinephrine regulation of AMPA-receptor trafficking. Cell 131:160–173.17923095
8. Dias-Ferreira E , Sousa JC , Melo I , Morgado P , Mesquita AR , Cerqueira JJ , et al. (2009): Chronic stress causes frontostriatal reorganization and affects decision-making. Science 325:621–625.19644122
9. Barik J , Marti F , Morel C , Fernandez SP , Lanteri C , Godeheu G , et al. (2013): Chronic stress triggers social aversion via glucocorticoid receptor in dopaminoceptive neurons. Science 339:332–335.23329050
10. de Quervain DJ , Roozendaal B , Nitsch RM , McGaugh JL , Hock C (2000): Acute cortisone administration impairs retrieval of long-term declarative memory in humans. Nat Neurosci 3:313–314.10725918
11. de Quervain DJ , Roozendaal B , McGaugh JL (1998): Stress and glucocorticoids impair retrieval of long-term spatial memory. Nature 394:787–790.9723618
12. Lupien SJ , McEwen BS (1997): The acute effects of corticosteroids on cognition: Integration of animal and human model studies. Brain Res Brain Res Rev 24:1–27.9233540
13. de Kloet ER (2014): From receptor balance to rational glucocorticoid therapy. Endocrinology 155:2754–2769.24828611
14. Finsterwald C , Alberini CM (2014): Stress and glucocorticoid receptor-dependent mechanisms in long-term memory: From adaptive responses to psychopathologies. Neurobiol Learning Memory 112:17–29.
15. Kaouane N , Porte Y , Vallee M , Brayda-Bruno L , Mons N , Calandreau L , et al. (2012): Glucocorticoids can induce PTSD-like memory impairments in mice. Science 335:1510–1513.22362879
16. Ni Y , Zhao X , Bao G , Zou L , Teng L , Wang Z , et al. (2006): Activation of beta2-adrenergic receptor stimulates gamma-secretase activity and accelerates amyloid plaque formation. Nat Med 12:1390–1396.17115048

17. Hara MR , Kovacs JJ , Whalen EJ , Rajagopal S , Strachan RT , Grant W , et al. (2011): A stress response pathway regulates DNA damage through beta2-adrenoreceptors and beta-arrestin-1. Nature 477:349–353.21857681
18. Dang V , Medina B , Das D , Moghadam S , Martin KJ , Lin B , et al. (2014): Formoterol, a long-acting beta 2 adrenergic agonist, improves cognitive function and promotes dendritic complexity in a mouse model of Down syndrome. Biol Psychiat 75:179–188.23827853
19. Gibbs M (2014): Reflections on glycogen and β-amyloid: Why does glycogenolytic β2-adrenoceptor stimulation not rescue memory after β-amyloid? Metabol Brain Dis 30:345–352.
20. Dong JH , Chen X , Cui M , Yu X , Pang Q , Sun JP (2012): Beta2-adrenergic receptor and astrocyte glucose metabolism. J Mol Neurosci 48:456–463.22399228
21. Catus SL , Gibbs ME , Sato M , Summers RJ , Hutchinson DS (2011): Role of beta-adrenoceptors in glucose uptake in astrocytes using beta-adrenoceptor knockout mice. Br J Pharmacol 162: 1700–1715.21138422
22. Hutchinson DS , Summers RJ , Gibbs ME (2007): Beta2- and beta3-adrenoceptors activate glucose uptake in chick astrocytes by distinct mechanisms: A mechanism for memory enhancement? J Neurochem 103:997–1008.17680985
23. Gibbs ME , Hutchinson DS , Summers RJ (2008): Role of beta-adrenoceptors in memory consolidation: Beta3-adrenoceptors act on glucose uptake and beta2-adrenoceptors on glycogenolysis. Neuropsychopharmacology 33:2384–2397.18046311
24. Gao V , Suzuki A , Magistretti PJ , Lengacher S , Pollonini G , Steinman MQ , Alberini CM (2016): Astrocytic beta2-adrenergic receptors mediate hippocampal long-term memory consolidation. Proc Natl Acad Sci U S A 113:8526–8531.27402767
25. LaForce C , Prenner BM , Andriano K , Lavecchia C , Yegen U (2005): Efficacy and safety of formoterol delivered via a new multidose dry powder inhaler (Certihaler) in adolescents and adults with persistent asthma. J Asthma 42:101–106.15871441
26. Suzuki A , Stern SA , Bozdagi O , Huntley GW , Walker RH , Magistretti PJ , Alberini CM (2011): Astrocyte-neuron lactate transport is required for long-term memory formation. Cell 144:810–823.21376239
27. Wang HM , Dong JH , Li Q , Hu Q , Ning SL , Zheng W , et al. (2014): A stress response pathway in mice upregulates somatostatin level and transcription in pancreatic delta cells through Gs and beta-arrestin 1. Diabetologia 57:1899–1910.24947582
28. Wisler JW , Xiao K , Thomsen AR , Lefkowitz RJ (2014): Recent developments in biased agonism. Curr Opin Cell Biol 27:18–24.24680426
29. Yang F , Yu X , Liu C , Qu CX , Gong Z , Liu HD , et al. (2015): Phosphoselective mechanisms of arrestin conformations and functions revealed by unnatural amino acid incorporation and (19)F-NMR. Nat Commun 6:8202.26347956
30. Daaka Y , Luttrell LM , Lefkowitz RJ (1997): Switching of the coupling of the beta2-adrenergic receptor to different G proteins by protein kinase A. Nature 390:88–91.9363896
31. Hu QX , Dong JH , Du HB , Zhang DL , Ren HZ , Ma ML , et al. (2014): Constitutive Galphai coupling activity of very large G protein-coupled receptor 1 (VLGR1) and its regulation by PDZD7 protein. J Biol Chem 289:24215–24225.24962568
32. Hase M , Yokomizo T , Shimizu T , Nakamura M (2008): Characterization of an orphan G protein-coupled receptor, GPR20, that constitutively activates Gi proteins. J Biol Chem 283:12747–12755.18347022
33. Shukla AK , Westfield GH , Xiao K , Reis RI , Huang LY , Tripathi-Shukla P , et al. (2014): Visualization of arrestin recruitment by a G-protein-coupled receptor. Nature 512:218–222.25043026
34. Bezzi P , Volterra A (2011): Astrocytes: Powering memory. Cell 144: 644–645.21376229
35. Zecchini V , Madhu B , Russell R , Pertega-Gomes N , Warren A , Gaude E (2014): Nuclear ARRB1 induces pseudohypoxia and cellular metabolism reprogramming in prostate cancer. EMBO J 33:1365–1382.24837709
36. Shenoy SK , Han S , Zhao YL , Hara MR , Oliver T , Cao Y , Dewhirst MW (2012): Beta-arrestin1 mediates metastatic growth of breast cancer cells by facilitating HIF-1-dependent VEGF expression. Oncogene 31:282–292.21685944

37. Liu X , Ma L , Li HH , Huang B , Li YX , Tao YZ , Ma L (2015): Beta-arrestin-biased signaling mediates memory reconsolidation. Proc Natl Acad Sci U S A 112:4483–4488.25831532

38. Lymperopoulos A , Negussie S (2013): betaArrestins in cardiac G protein-coupled receptor signaling and function: Partners in crime or "good cop, bad cop"? Int J Mol Sci 14:24726–24741.24351844

39. Capote LA , Mendez Perez R , Lymperopoulos A (2015): GPCR signaling and cardiac function. Eur J Pharmacol 763:143–148.25981298

40. Srivastava A , Gupta B , Gupta C , Shukla AK (2015): Emerging functional divergence of beta-arrestin isoforms in GPCR function. Trends Endocrinol Metab 26:628–642.26471844

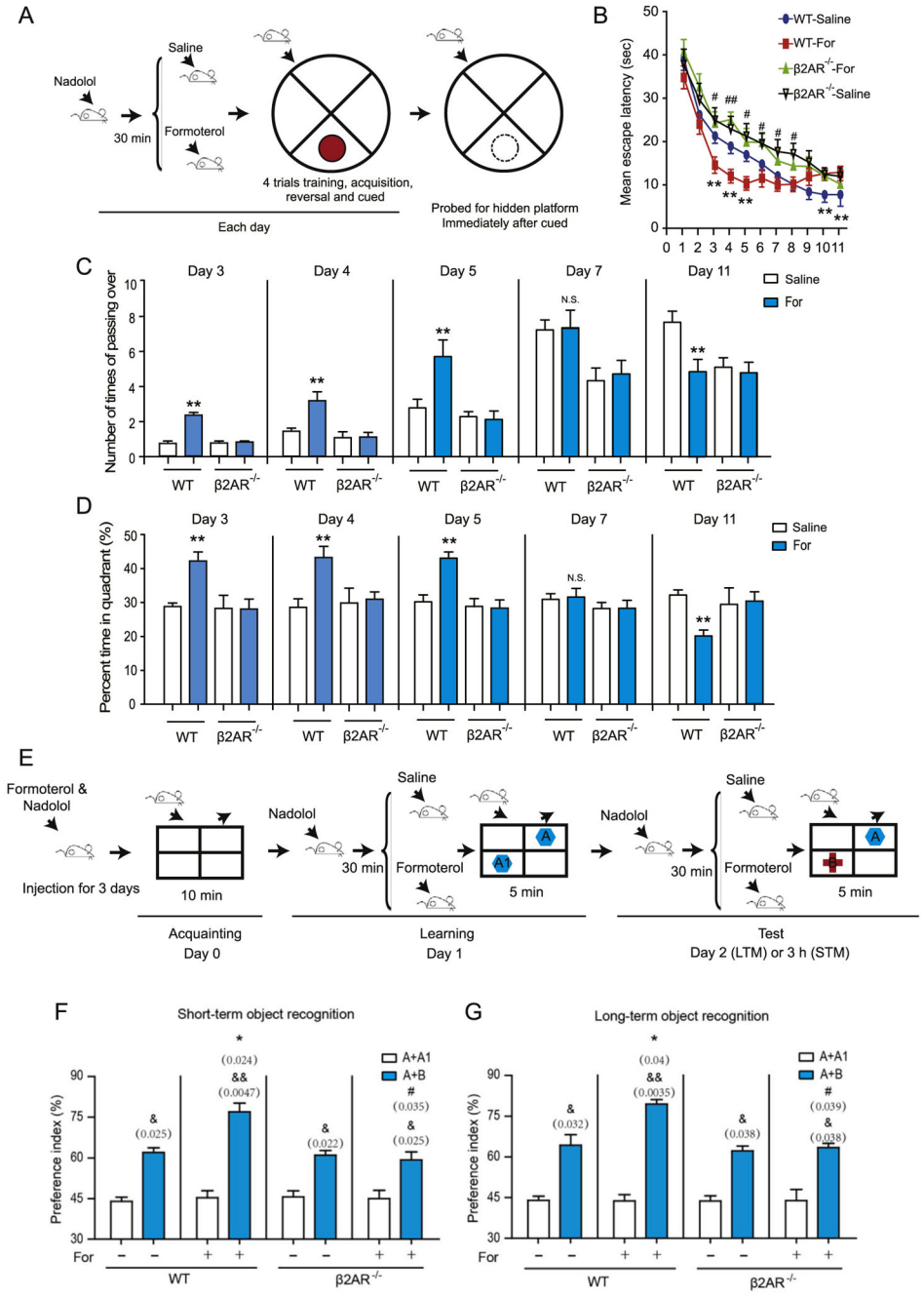

Figure 1.

The duration of β_2-adrenergic receptor (β2AR) activation determines the consequences for learning ability. **(A)** Experimental protocols for the Morris water maze experiments. The mean escape latency (seconds) of mice was measured during all 11 days of training. Each day, the animals were first treated with the βAR antagonist nadolol (5 mg/kg, intraperitoneal) and then administered the β2AR agonist formoterol (For) (2 mg/kg, intraperitoneal) before the behavioral tests (upper panel). **(B)** Formoterol administration caused a significantly shorter mean escape latency on days 3, 4, and 5 compared with wild-type (WT) mice (n = 20 for each group). However, on days 10 and 11, continued

administration of formoterol led to a significantly longer mean escape latency. The β2AR$^{-/-}$ mice (n = 10 for each group) on formoterol showed no significant differences from the β2AR$^{-/-}$ mice on the vehicle, and both groups had a longer mean escape latency compared with their formoterol-treated WT-mouse littermates after 3 days (**(left to right) p = .0483, p = .0375, p = .0481, p = .0492, p = .0387; $^{\#}p$ = .0115; $^{\#\#}p$ = .0098; $^{\#}p$ = .0321, p = .0167, p = .01009, p = .02610). **(C)** Bar graphs depict the number of crosses over the hidden platform location during the Morris water maze experiments. Compared with saline-treated mice, formoterol-treated WT mice had significantly more crossing times on days 3, 4, and 5; no significant differences on day 7; and significantly fewer crossing times on day 11. The effect of formoterol on crossing time was abolished in the β2AR$^{-/-}$ mice (**p = .0028, p = .0054, p = .0074, p = .0082). **(D)** Bar graphs depict the mean percentage of time spent in the correct quadrant after completion of the last learning trial. Mice were placed in the opposite quadrant, and the platform was removed in the target quadrant before starting the experiments. Compared with saline-treated mice, WT mice treated with formoterol spent significantly more time in the correct quadrant on days 3, 4, and 5, but significantly less time on day 11 (**p = .0093, p = .0098, p = .0087, p = .0091). **(E)** The graph depicts the experimental protocols for the object recognition task. For the adaptive β2AR activation, mice were continuously administered formoterol/nadolol for 3 days, as depicted in **(A)**, before the recognition task. Experimental details for the recognition task are presented in the Supplemental Methods. **(F, G)** Object recognition task. Bar graphs depict the preference index (PI) of the object preferences, which is evaluated 3 and 24 hours after the initial familiarization trial. WT mice treated with formoterol showed a significantly higher PI compared with mice treated with saline, whereas β2AR$^{-/-}$ mice had no significant differences in PI (n = 10 for each group; **(F)** *p = .024; $^{\#}p$ = .035, $^{\&}p$ = .025; $^{\&\&}p$ = .0047; $^{\&}p$ = .022, p = .025; **(G)** *p = .04, $^{\#}p$ = .039, $^{\&}p$ = .032, $^{\&\&}p$ = .0035, $^{\&}p$ = .038, p = .038). **(B–D, F, G)** *p < .05, **p < .01, WT-mice administered formoterol were compared to the saline group; $^{\#}p$ < .05, $^{\#\#}p$ < .01; β2AR$^{-/-}$ mice treated with formoterol were compared with WT mice treated with formoterol. $^{\&}p$ < .05, $^{\&\&}p$ < .01; the PI before or after training was compared. LTM, long-term memory; N.S., not significant; STM, short-term memory.

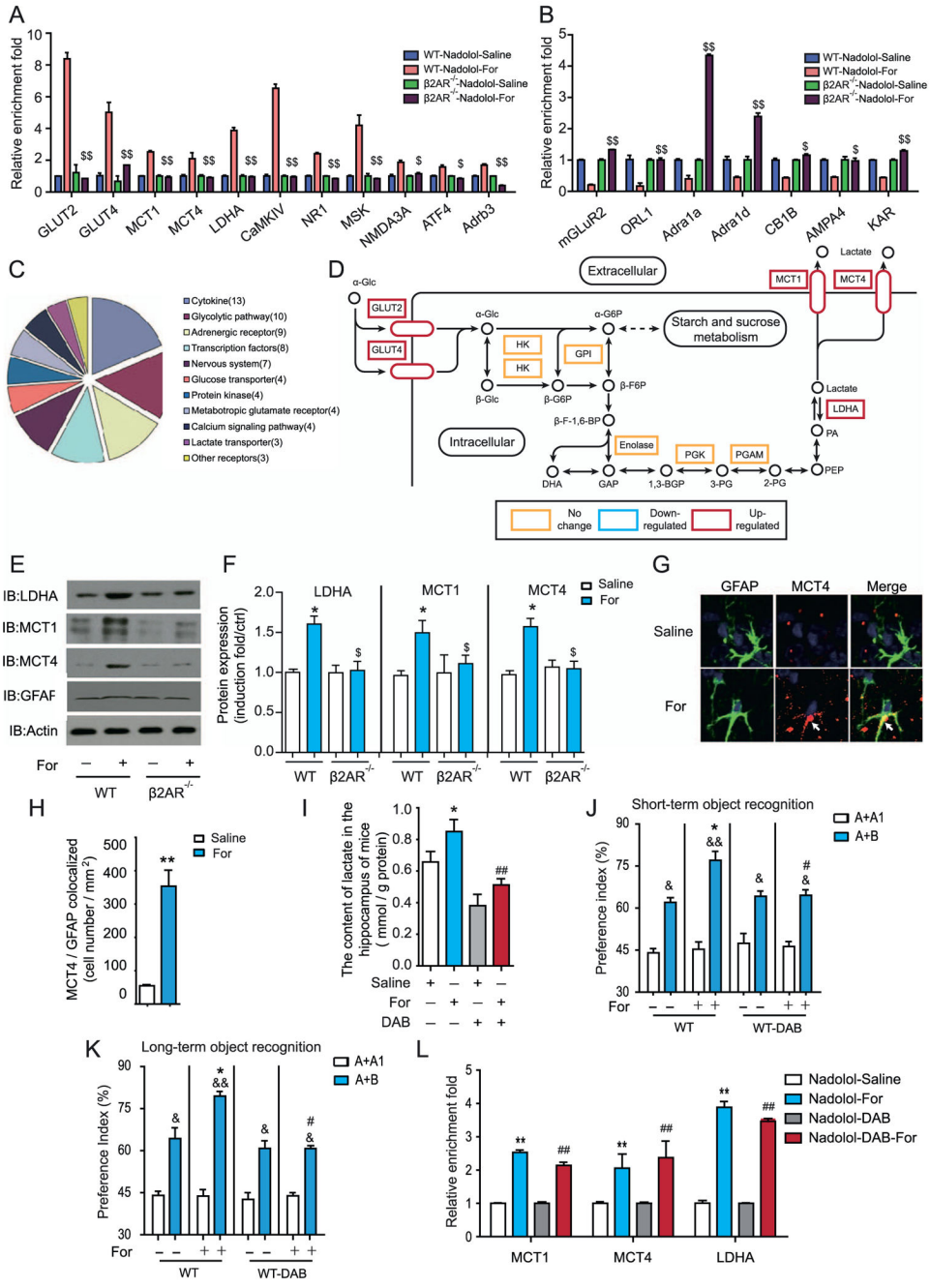

Figure 2.

Activation of β_2-adrenergic receptors (β2ARs) promotes astrocyte-neuron lactate transport, which is required for increased learning ability. **(A, B)** Quantitative reverse transcriptase polymerase chain reaction (QRTPCR) analysis of the messenger RNA (mRNA) transcription profiles of genes important for learning and memory after formoterol (For) stimulation for 3 days in wild-type (WT) or $\beta2AR^{-/-}$ mice. **(A)** After continuous formoterol administration, mRNA levels of the genes showed an increase in the WT but not in the $\beta2AR^{-/-}$ mice. **(B)** mRNA levels of the genes showed a decrease in WT mice but were abolished in $\beta2AR^{-/-}$ mice. Expression levels were normalized to actin levels. **(C)** The graph represents the

clustering of the 69 important learning and memory genes that were examined (in **[A]**) into subfunctional groups. **(D)** Activation of β2ARs in the hippocampus upregulates the expression of several key genes in the lactate metabolism and transport subnetworks. Gene transcription with significant increases is shown in the red rectangle, and genes with no significant changes are shown in the yellow rectangle. **(E, F)** Activation of β2ARs by formoterol increased protein levels of lactate dehydrogenase A (LDHA), monocarboxylate transporter 1 (MCT1), and MCT4 in the hippocampus of WT mice but not $\beta2AR^{-/-}$ mice. **(E)** Representative Western blots for MCT1, MCT4, and LDHA in the hippocampus from WT or $\beta2AR^{-/-}$ mice. **(F)** Bands from Western blots (performed in triplicate as a minimum) were quantified and expressed as induction folds over the control **(E)** ($^{*}p = .037$, $p = .04$, $p = .016$; $^{\$}p = .021$, $p = .048$, $p = .027$). **(G)** Representative immunostaining image of MCT4 in the hippocampus with/without formoterol treatment for 3 days. **(H)** Statistical analysis and a bar graph represent the colocalization of MCT4 expression with glial fibrillary acidic protein (GFAP) in **(G)** and Supplemental Figure S9. $n = 6$ mice per group; four random areas were picked out from each hippocampus section, and five sections were randomly selected from each mouse. The colocalization of MCT4 with the marker of the astrocytes (GFAP) was significantly increased after formoterol treatment. **(I)** Formoterol administration increased lactate levels in the hippocampus, which is blocked by the inhibitor of glycogen phosphorylation DAB. **(J, K)** Improved object preference in recognition memory after formoterol administration was abolished by 1,4-dideoxy-1,4-imino-D-arabinitol (DAB) treatment ($n = 10$ for each group: **[J]** $^{*}p = .036$, $^{\#}p = .036$, $^{\&}p = .033$, $^{\&\&}p = .006$, $^{\&}p = .03$, $p = .04$; **[K]** $^{*}p = .035$, $^{\#}p = .04$, $^{\&}p = .03$; $^{\&\&}p = .0029$; $^{\&}p = .04$, $p = .04$). **(L)** QRTPCR analysis of mRNA transcription profiles of genes important for learning and memory after saline, formoterol, DAB, and formoterol and DAB stimulation for 3 days in WT mice. Results show that DAB application has no significant effect on mRNA levels of MCT1, MCT4, and LDHA. Data were normalized to actin levels. **(A–L)** All animal experiments were performed with at least six animals in each group. $^{*}p < .05$; $^{***}p < .005$; formoterol-treated animals were compared with control vehicle-treated animals. $^{\#}p < .05$; DAB-treated animals were compared with control vehicle-treated animals. $^{\$}p < .05$, $^{\$\$}p < .01$; $\beta2AR^{-/-}$ mice were compared with their WT littermates. $^{\&}p < .05$, $^{\&\&}p < .01$; preference indexes before and after training were compared. All data were analyzed with one- or two-way analysis of variance. Adra1a, adrenergic receptor, alpha 1a; Adra1d, adrenergic receptor, alpha 1d; Adrb3, adrenergic receptor, beta 3; AMPA4, glutamate receptor, ionotropic, alpha-amino-3-hydroxy-5-methyl-4-isoxazolpropionate receptor 4; ATF4, activating transcription factor 4; CaMKIV, calcium/calmodulin-dependent protein kinase IV; CB1B, cannabinoid receptor 1; ctrl, control; GPI, glucose phosphate isomerase; HK, hexokinase; IB, immunoblot; KAR, voltage-sensitive potassium/chloride channel; mGLuR2, metabotropic glutamate receptor 2 (G-protein-coupled receptor type); MSK, mitogen and stress activated protein kinase; NMDA3A, *N*-methyl-D-aspartate receptor 3A (glutamate receptor, ion channel type); NR1, ionotropic, *N*-methyl-D-aspartate receptor channel, subunit zeta-1 (glutamate receptor, ion channel type); ORL-1, opioid receptor-like 1; PGAM, phosphoglycerate mutase; PGK, phosphoglycerate kinase.

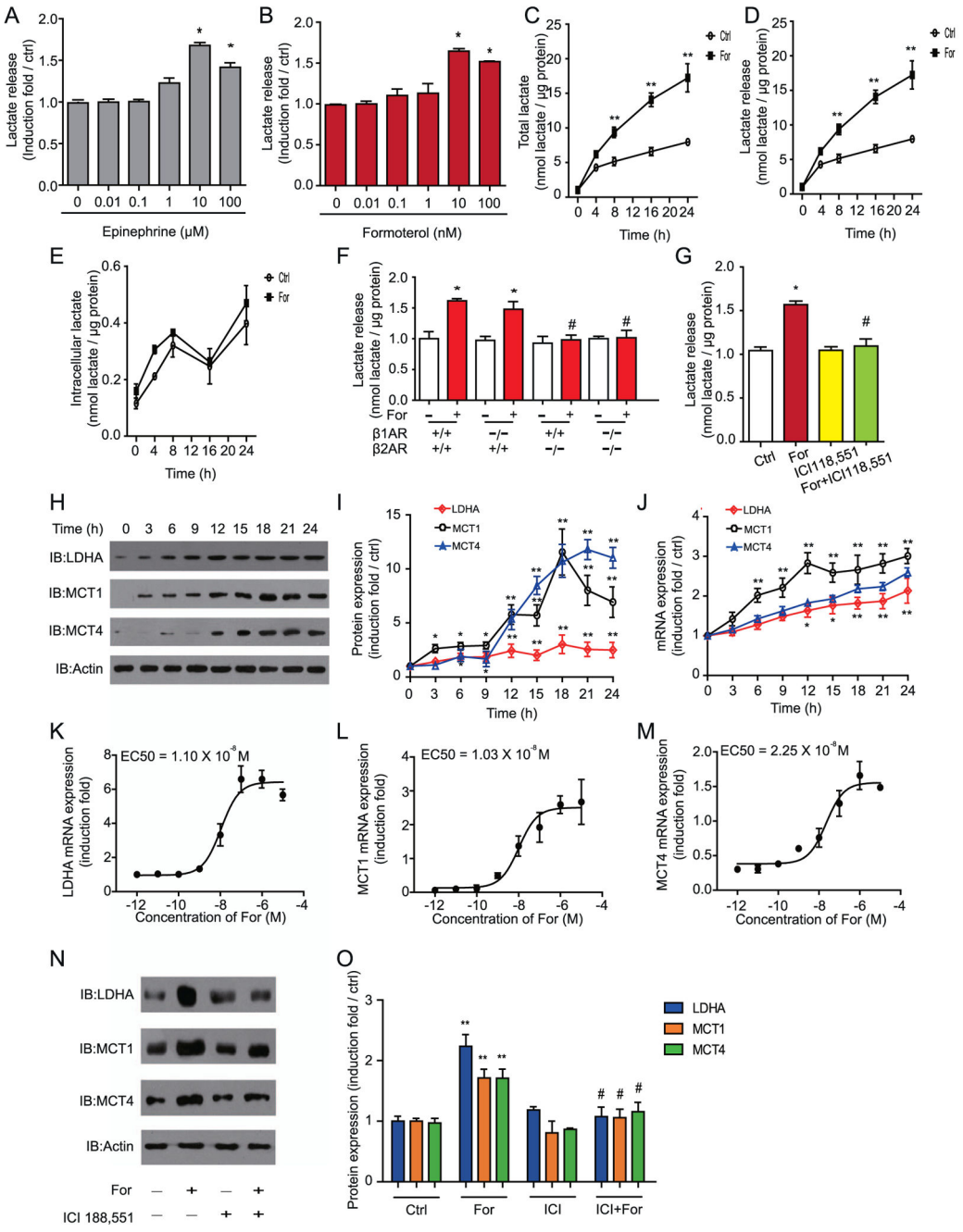

Figure 3.

Activation of β_2-adrenergic receptor (β2AR) promotes lactate synthesis and transport and increases expression of key elements in the lactate metabolism in astrocytes in a dose- and time-dependent manner. **(A, B)** The β2AR agonists **(A)** formoterol (For) and **(B)** epinephrine induced lactate release in a dose-dependent manner. Cells were treated with 0, 0.01, 0.1, 1, 10, and 100 μmol/L of epinephrine (left panel) or 0, 0.01, 0.1, 1, 10, and 100 nmol/L of formoterol (right panel) separately for 16 hours. Data are averages of at least three independent experiments and are presented as induction folds over control (Ctrl) levels. **(C–E)** Formoterol promoted lactate synthesis and transportation in U251 cells. **(C)** Total lactate

amount, **(D)** lactate release, and **(E)** intracellular lactate levels were measured after cells were treated with 10 nmol/L of formoterol. The y-axis represents the concentration of lactate (nmol) over the total amount of protein (μg). The solid line depicts data from cells infused with formoterol, and the dashed line depicts control data. Data are averages of at least three independent experiments. **(F)** Formoterol promoted lactate release through β2AR. Primary cultured mouse astrocytes from $\beta1AR^{-/-}$, $\beta2AR^{-/-}$, and $\beta1AR^{-/-}/\beta2AR^{-/-}$ mice and their wild-type littermates were treated with or without 10 nmol/L of formoterol for 16 hours. The y-axis represents lactate release in the treated groups vs. control. **(G)** The effect of selective β2AR antagonists on the response to formoterol in astrocytes. The column represents the induction folds of lactate release over the control. **(H, I)** Activation of βARs by formoterol increased protein levels of lactate dehydrogenase A (LDHA), monocarboxylate transporter 1 (MCT1), and MCT4 in a time-dependent manner. **(H)** Representative Western blot images of LDHA, MCT1, and MCT4. **(I)** Bands from Western blots (performed in triplicate as a minimum) were quantified and expressed as induction folds over control (LDHA, $*p = .049$, $p = .047$, $**p = .008$, $p = .009$, $p = .005$, $p = .006$, $p = .005$; MCT1, $*p = .025$, $p = .019$, $p = .017$, $**p = .006$, $p = .0058$, $p = .0072$, $p = .0066$, $p = .0058$; MCT4, $*p = .013$, $p = .025$, $**p = .0083$, $p = .0064$, $p = .0077$, $p = .0069$, $p = .0062$). **(J)** Formoterol increased messenger RNA (mRNA) LDHA, MCT1, and MCT4 levels in a time-dependent manner, as examined by quantitative reverse transcriptase polymerase chain reaction. **(K–M)** Concentration-dependent effects of formoterol (12 hours) on LDHA, MCT1, and MCT4 mRNA levels in U251 cells. **(N, O)** Formoterol-stimulated LDHA, MCT1, and MCT4 protein expression increases through activation of β2ARs. **(N)** Representative Western blot images of LDHA, MCT1, and MCT4. Western bands from at least triplicate experiments, as shown in **(N)**, were quantified and are shown as induction folds over the control in **(O)** ($**p = .0074$, $p = .0087$, $p = .009$; $^{\#}p = .018$, $p = .017$, $p = .012$). **(A–O)** All data points were obtained from mean values (±SEM) of at least three independent samples. $*p < .05$; $**p < .01$; agonist-treated samples were compared with nontreated samples. $^{\#}p < .05$; $\beta1AR^{-/-}/\beta2AR^{-/-}$ mice were compared with WT mice, and antagonist (ICI 118,551)-treated samples were compared with cells treated with formoterol only. EC50, concentration for 50% of maximal effect; IB, immunoblot.

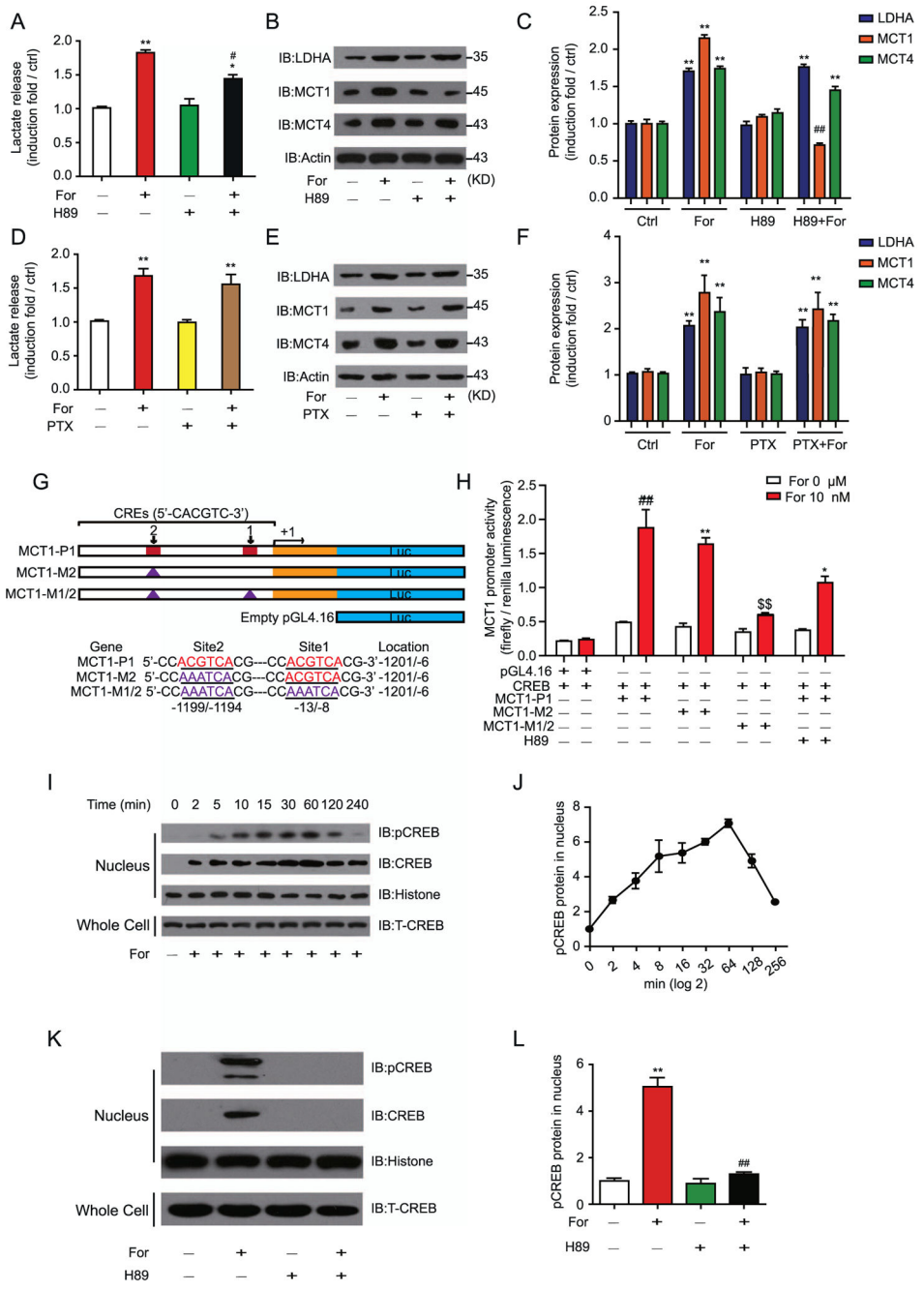

Figure 4.

The β_2-adrenergic receptor (β2AR)–Gs-protein kinase A (PKA)-phosphorylated cyclic adenosine monophosphate response element binding protein (pCREB) signaling pathway regulates monocarboxylate transporter 1 (MCT1) transcription and lactate release. **(A)** The PKA inhibitor H89 (2 μmol/L) inhibited formoterol (For)-induced lactate release in U251 cells. U251 cells were infused with formoterol with or without inhibition by H89 for 12 hours. **(B, C)** Gs-PKA signaling regulated MCT1 expression in U251 cells downstream of β2AR. Cells were treated with formoterol (10 nmol/L) for 16 hours. The effect of H89 on formoterol-induced lactate dehydrogenase A (LDHA), MCT1, and MCT4 expression was

monitored by **(B)** Western blots and **(C)** quantified (**p = .0051, p = .0054, p = .0052, p = .0049, p = .005; $^{\#\#}p$ = .0036). **(D)** The effect of the inhibitory G protein (Gi) inhibitor pertussis toxin (PTX) (100 ng/mL) on formoterol-induced lactate release in U251 cells. U251 cells were preincubated with PTX for 16 hours, then formoterol (10 nmol/L)–induced lactate release was examined. **(E, F)** Cells were preincubated with PTX (100 ng/mL), then treated with formoterol for 16 hours. The effect of PTX on formoterol-induced LDHA, MCT1, and MCT4 expression levels were **(E)** evaluated by Western blots and **(F)** quantified (**p = .0075, p = .0067, p = .0083, p = .0079, p = .0081, p = .0078). **(G)** The scheme depicts the putative CREB binding site (CRE) in the promoter sequence of human MCT1 (21928/100). The wild-type promoter and the promoter with different mutations (site 1 or site 2) were cloned into the pGL4.16 vector. An empty pGL4.16 vector was used as a negative control (ctrl). Exon 1 is shown by the yellow rectangle, and the mutation site is shown by the blue triangle. **(H)** β2AR-Gs-PKA signaling regulated MCT1 transcription mainly through the binding of CREB to the promoter sites. Formoterol-induced wild-type or mutated MCT1 promoter activity was assayed by luciferase activity. The effect of H89 was also examined. Expression of the firefly luciferase reporter gene was used to determine the promoter activity. **(I, J)** Formoterol increased CREB phosphorylation levels in U251 cells. Representative **(I)** Western blots and **(J)** statistical analysis show pCREB levels at different time points in U251 cells that were administered formoterol. **(K, L)** β2AR-Gs-PKA signaling regulated CREB phosphorylation in U251 cells. Phospho-CREB levels in nuclei of U251 cells treated with formoterol with or without H89 inhibition are shown. **(K)** Representative Western blot image; **(L)** statistical analysis (**p = .0019; $^{\#\#}p$ = .0023). **(A–I)** Representative Western blots from at least three independent experiments are shown and quantified. All statistical data are mean values (6SEM) of at least three independent experiments. *p < .05; **p < .01; formoterol-treated samples were compared with nontreated samples. H89-treated (or PTX-treated) samples were compared with non–H89-treated (or non-PTX-treated) samples. $^{\$\$}p$ < .01; $^{\$\$\$}p$ < .005 mutations of MCT1 promoters were compared with the wild-type MCT1 promoter. IB, immunoblot; T-CREB, total CREB.

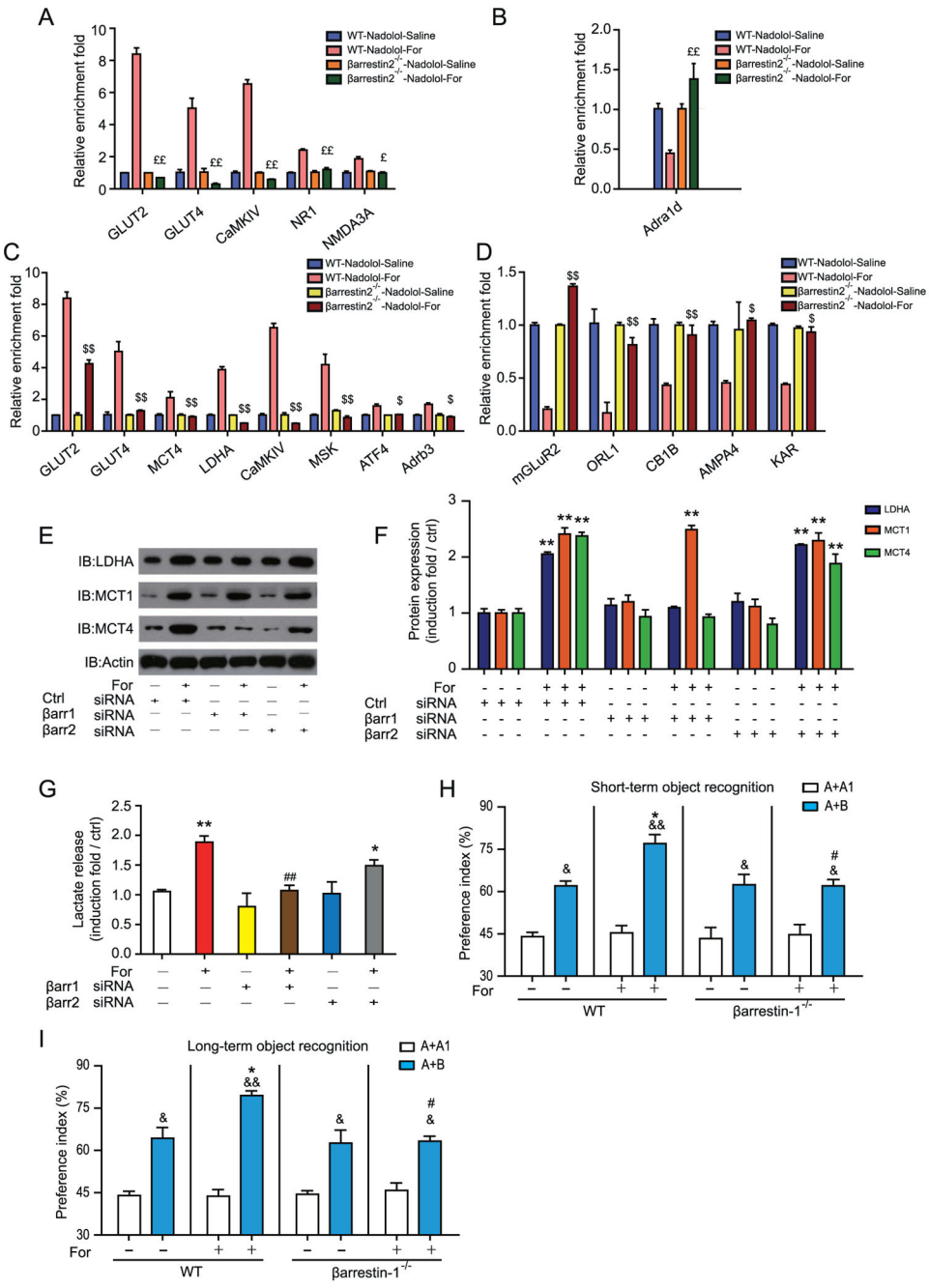

Figure 5.

β-Arrestin-1 (βarr1) is required for increased lactate metabolism and improved learning ability after β_2 adrenergic receptor (β2AR) activation. **(A, B)** Quantitative reverse transcripase polymerase chain reaction (QRTPCR) analysis of messenger RNA (mRNA) levels after formoterol (For) stimulation for 3 days in βarr2$^{-/-}$ mice and their wild-type (WT) littermates. Only genes that are downstream of the β2AR activation were examined. mRNA levels of genes that showed **(A)** an increase in the WT but not βarr2$^{-/-}$ mice and **(B)** a decrease in WT mice but in βarr2$^{-/-}$ mice. Expression levels were normalized to actin levels. **(C, D)** Similar to **(A, B)**, QRTPCR analysis of mRNA levels after formoterol

stimulation in WT or βarr1$^{-/-}$ mice. **(C, D)** mRNA levels of genes that showed **(C)** an increase or **(D)** decrease in WT mice, but not in βarr1$^{-/-}$ mice. **(E, F)** βarr1 mediated lactate dehydrogenase A (LDHA) and monocarboxylate transporter 4 (MCT4) expression after β2AR activation. **(E)** Representative Western blots of cells treated with (or without) formoterol. **(F)** Statistical data from at least three independent experiments (**p = .0027, p = .0025, p = .0021, p = .0023, p = .0022, p = .0020, p = .0027). **(G)** βarr1 is required in formoterol-induced lactate release in U251 cells. Lactate release in U251 cells transfected with control small interferring RNA (siRNA) or siRNA targeted to βarr1 or βarr2. Cells were treated with or without formoterol for 16 hours (n = 3). **(H, I)** βarr1 is required for improvement of the object preference after formoterol administration. Object preference was assessed as described in Figure 1E. WT mice treated with formoterol displayed significantly higher discrimination ratios compared with mice treated with saline, whereas βarr1$^{-/-}$ mice showed no significant difference between the formoterol-treated and saline-treated groups (n = 8 for each group) (n = 10 for each group; **(H)** *p = .035, $^{\#}p$ = .047, $^{\&}p$ = .025, $^{\&\&}p$ = .0035, $^{\&}p$ = .024, p = .024; **(I)** * p = .032, $^{\#}p$ = .03, $^{\&}p$ = .033; $^{\&\&}p$ = .0029; $^{\&}p$ = .039, p = .032). **(A–H)** *p < .05; **p < .01; cells treated with formoterol were compared with the saline group. $^{\#}p$ < .05; $^{\#\#}p$ < .01; βarr1 or βarr2 siRNA–treated cells were compared with control (Ctrl) siRNA-treated cells. $^{\$}p$ < .05; $^{\$\$}p$ < 0.01; βarr1$^{-/-}$ mice were compared with their WT littermates. $^{£}p$ < .05; $^{££}p$ < .01; βarr2$^{-/-}$ mice were compared with their WT littermates. $^{\&}p$ < .05, $^{\&\&}p$ < .01; preference indexes before and after training were compared. Adra1d, adrenergic receptor, alpha 1d; Adrb3, adrenergic receptor, beta 3; AMPA4, glutamate receptor, ionotropic, alpha-amino-3-hydroxy-5-methyl-4-isoxazolpropionate receptor 4; ATF4, activating transcription factor 4; CaMKIV, calcium/calmodulin-dependent protein kinase IV; CB1B, cannabinoid receptor 1; GLUT2, glucose transporter 2; IB, immunoblot; KAR, voltage-sensitive potassium/chloride channel; mGLuR2, metabotropic glutamate receptor 2 (G-protein-coupled receptor type); MSK, mitogen and stress activated protein kinase; NMDA3A, *N*-methyl-D-aspartate receptor 3A (glutamate receptor, ion channel type); NR1, ionotropic, *N*-methyl-D-aspartate receptor channel, subunit zeta-1 (glutamate receptor, ion channel type); ORL1, opioid receptor-like 1.

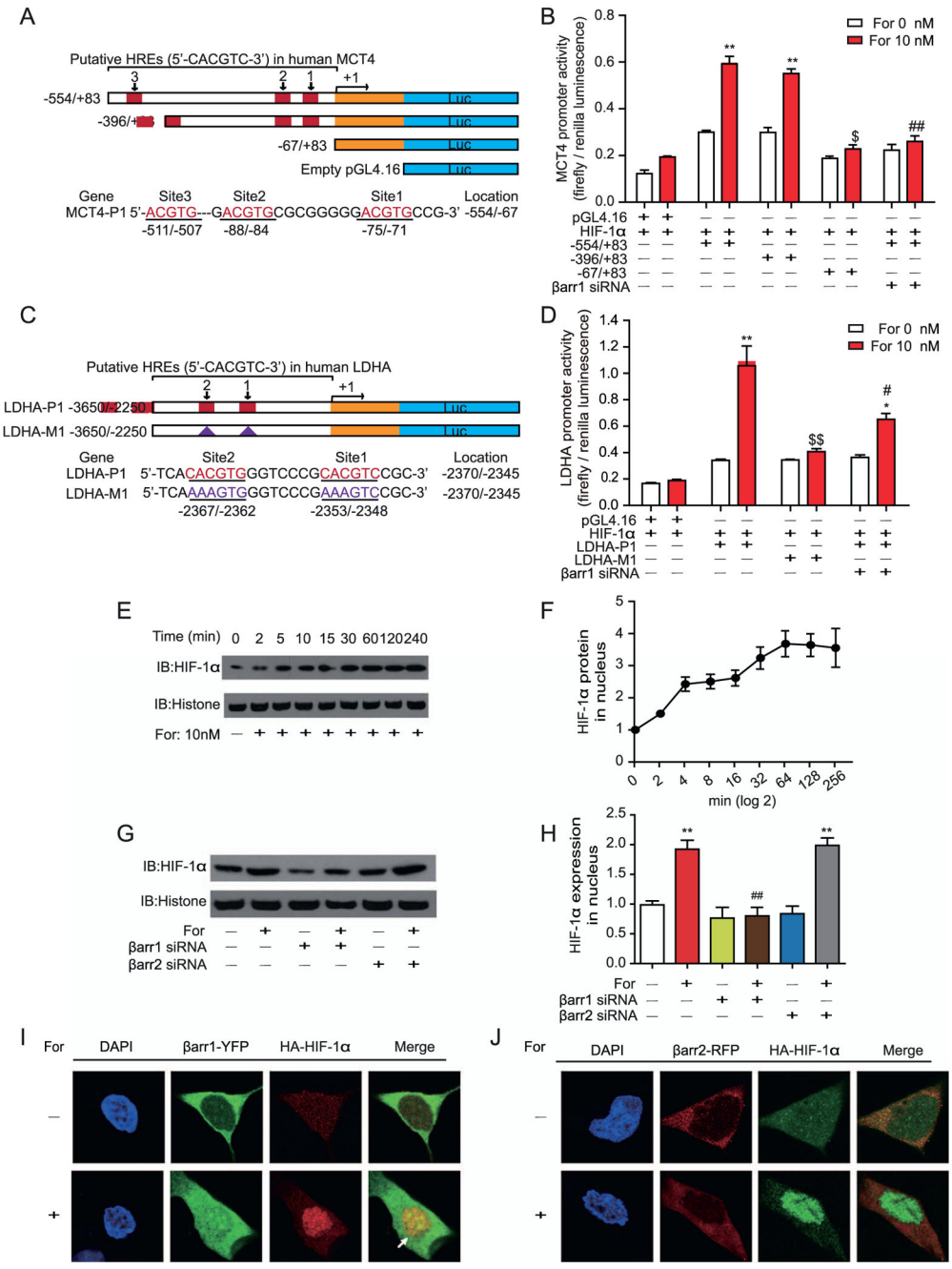

Figure 6.

Activation of β_2-adrenergic receptor (β2AR) regulates monocarboxylate transporter 4 (MCT4) and lactate dehydrogenase A (LDHA) transcription through translocation of hypoxia-inducible factor-1α (HIF-1α) into the nucleus. **(A, B)** Deletion analysis of human MCT4 promoters on the 5′-flanking sequences. **(A)** The scheme depicts promoter sequences with different hypoxia-response elements (HREs) that were cloned into a pGL4.16 vector, and the firefly luciferase reporter gene was expressed to determine promoter activity. **(A)** HRE sites are defined as 5′-ACGTG-3′, and the locations are indicated. Serial 5′ deletions of the full-length MCT4 promoters (−554/83) were generated by polymerase chain reaction.

The yellow rectangle represents the exon. **(B)** β2AR–β-arrestin-1 (βarr1) signaling regulated MCT4 transcription through the binding of HIF-1α to the promoter sites. Formoterol (For)-induced wild-type and truncated MCT4 promoter activity were assayed by luciferase activity. The contribution of βarr1 was monitored by βarr1 small interferring RNA (siRNA). **(C)** The scheme represents the HRE binding site on the LDHA promoter. Two HIF-1α binding sites were identified upstream of the transcriptional starting site. Mutations of the HIF-1α binding sites were designated as LDHA-M1. **(D)** β2AR-βarr1 signaling regulated LDHA transcription through HIF-1α. Formoterol-induced wild-type or mutated LDHA promoter activity was assayed by luciferase activity. Mutations of the HIF-1α binding site or knockdown of βarr1 significantly decreased LDHA transcriptional activation. **(E, F)** Nucleus HIF-1α levels at different time points were **(E)** demonstrated by Western blots and **(F)** subjected to statistical analysis. Cells were treated with 10 nmol/L of formoterol for the indicated time. **(G, H)** βarr1 is required for the formoterol-induced nuclear translocation of HIF-1α. **(G)** Representative Western blot images and **(H)** statistical analysis. Cells were transfected with control siRNA, βarr1 or βarr2 targeting siRNA before formoterol treatment (**$p = .0022$, $p = .0027$; $^{\#\#}p = .0033$). **(I, J)** Localizations of HIF-1α and βarr1/βarr2 with or without formoterol stimulation. Confocal images show **(I)** βarr1, HIF-1α (green and red), and **(J)** βarr2, HIF-1α (red and green) from cells treated with dimethyl sulfoxide (DMSO) (control) or 10 nmol/L of formoterol. There were few colocalizations between βarr1/βarr2 and HIF-1α in cells treated with DMSO. Formoterol treatment induced the colocalization of HIF-1α and βarr1. **(A–J)** At least three independent experiments were performed for all statistical analyses. *$p < .05$; formoterol-treated samples were compared with control vehicles. $^{\#}p < .05$; $^{\#\#}p < .01$; β-arrestin siRNA was compared with control siRNA, and mutated promoters were compared with wild-type promoters. $^{\$}p < .05$; $^{\$\$}p < 0.01$; mutations/deletions of MCT4/LDHA promoters were compared with wild-type MCT1/LDHA promoters. **(E, F)** Representative Western blots from at least three independent experiments are shown and quantified. DAPI, 4′,6-diamidino-2-phenylindole; HA, hemagglutinin antigen; IB, immunoblot; RFP, red fluorescent protein; YFP, yellow fluorescent protein.

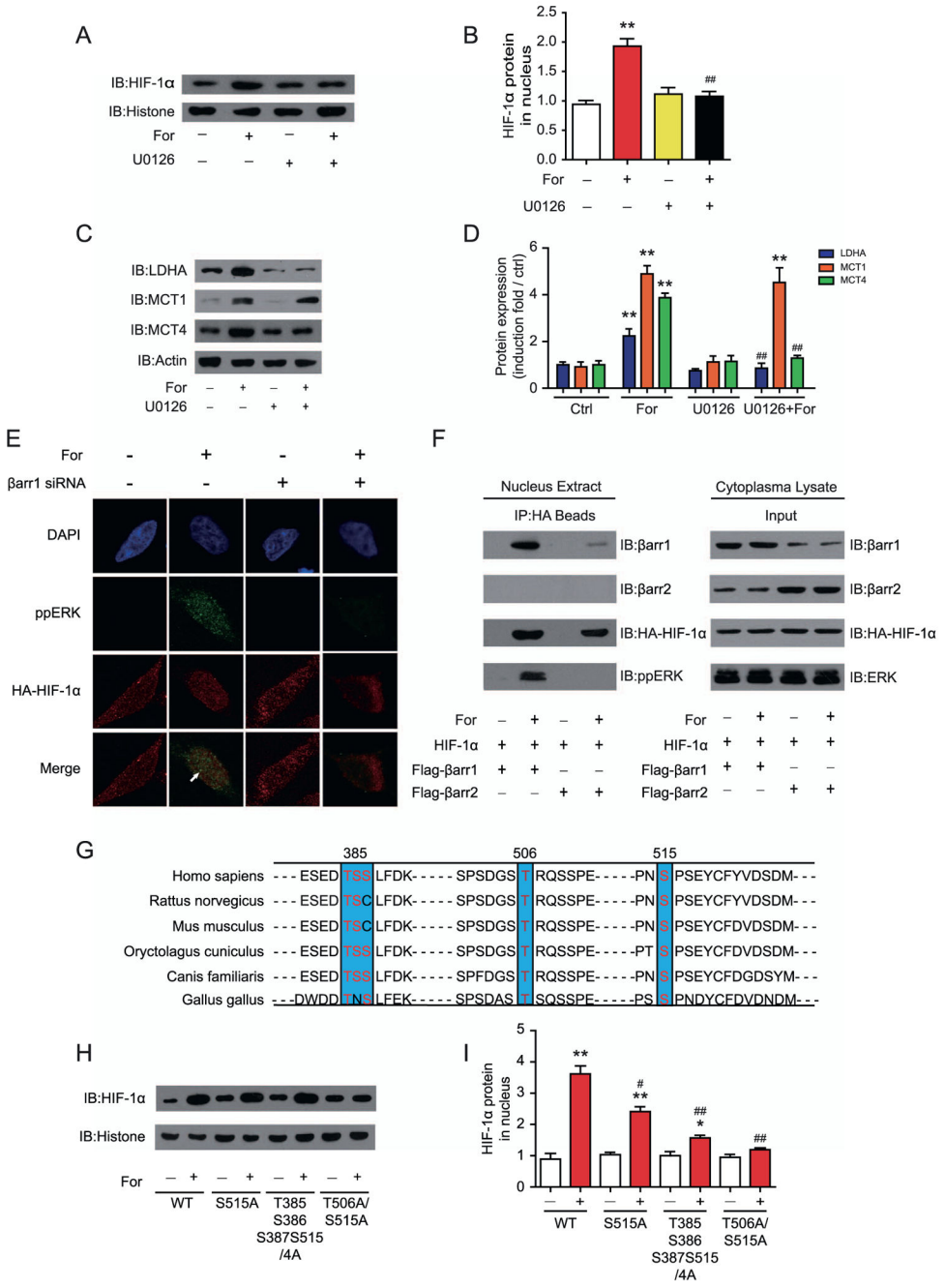

Figure 7.

Activation of β_2-adrenergic receptor (β2AR) leads to formation of a β-arrestin-1 (βarr1)-mitogen-activated protein kinase (ERK)-hypoxia-inducible factor-1α (HIF-1α) ternary complex and phosphorylation of HIF-1α at the T506 and S515 positions, which are required for HIF-1α retention in the nucleus. **(A, B)** ERK activation is required for the translocation of HIF-1α after β2AR activation. U251 cells were treated with or without the specific MEK inhibitor butanedinitrile, 2,3-bis[amino[(2-aminophenyl)thio]methylene] (U0126) before formoterol (For) treatment. **(A)** Representative Western blots for nucleus HIF-1α levels and **(B)** the statistical analysis (**p = .0035; $^{\#\#}p$ = .0041). **(C, D)** Effects of the MEK inhibitor

U0126 on formoterol-induced lactate dehydrogenase A (LDHA), monocarboxylate transporter 1 (MCT1), and MCT4 expression in U251 cells. **(C)** Representative Western blots, and **(D)** the statistical analysis (**p = .0031, p = .0017, p = .0026, p = .0021; $^{\#\#}p$ = .0045, p = .0041). **(E)** Colocalization of phospho-ERK (ppERK, green) and HIF-1β (red) in the nucleus after formoterol stimulation. Cells in the left panel were preincubated with control (Ctrl) small interferring RNA (siRNA), and cells in the right panel were preincubated with βarr1 siRNA. **(F)** Nuclear extracts of astrocytes cotransfected with hemagglutinin antigen (HA)-HIF-1α and Flag-βarr1/2 were prepared with or without formoterol treatment for 1 hour. Formation of the βarr1-ERK-HIF-1α ternary complex was analyzed by the immunoprecipitation of HA-HIF-1α, and βarr1, βarr2, and pp-ERK were detected in the immunoprecipitated complex with specific antibodies. **(G)** Sequence alignment of the potential ERK phosphorylation sites in HIF-1β between different species. **(H, I)** Effects of HIF-1β mutations on formoterol-induced HIF-1β translocation. Wild-type (WT) HIF-1α or HIF-1α S515A, T385S385S387S515/4A, and T506A/S515A were transfected into U251 cells. **(H)** After formoterol stimulation for 1 hour, the nucleus extract was prepared, and the presence of HIF-1α in the nucleus was examined by Western blot. **(I)** Statistical and bar graph representation of Western blot bands from **(H)** (**p = .0021, p = .004; *p = .015; $^{\#}p$ = .044, $^{\#\#}p$ = .0068, p = .0029). **(A–I)** Representative Western blots from at least three independent experiments are shown. At least three independent experiments were performed for all statistical analyses. *$p < .05$; formoterol-treated samples were compared with control vehicle samples. $^{\#}p < .05$; $^{\#\#}p < .01$; U0126-treated cells were compared with control cells, and cells transfected with the HIF-1β mutant were compared with cells transfected with the HIF-1β WT. DAPI, 4′,6-diamidino-2-phenylindole; IB, immunoblot.

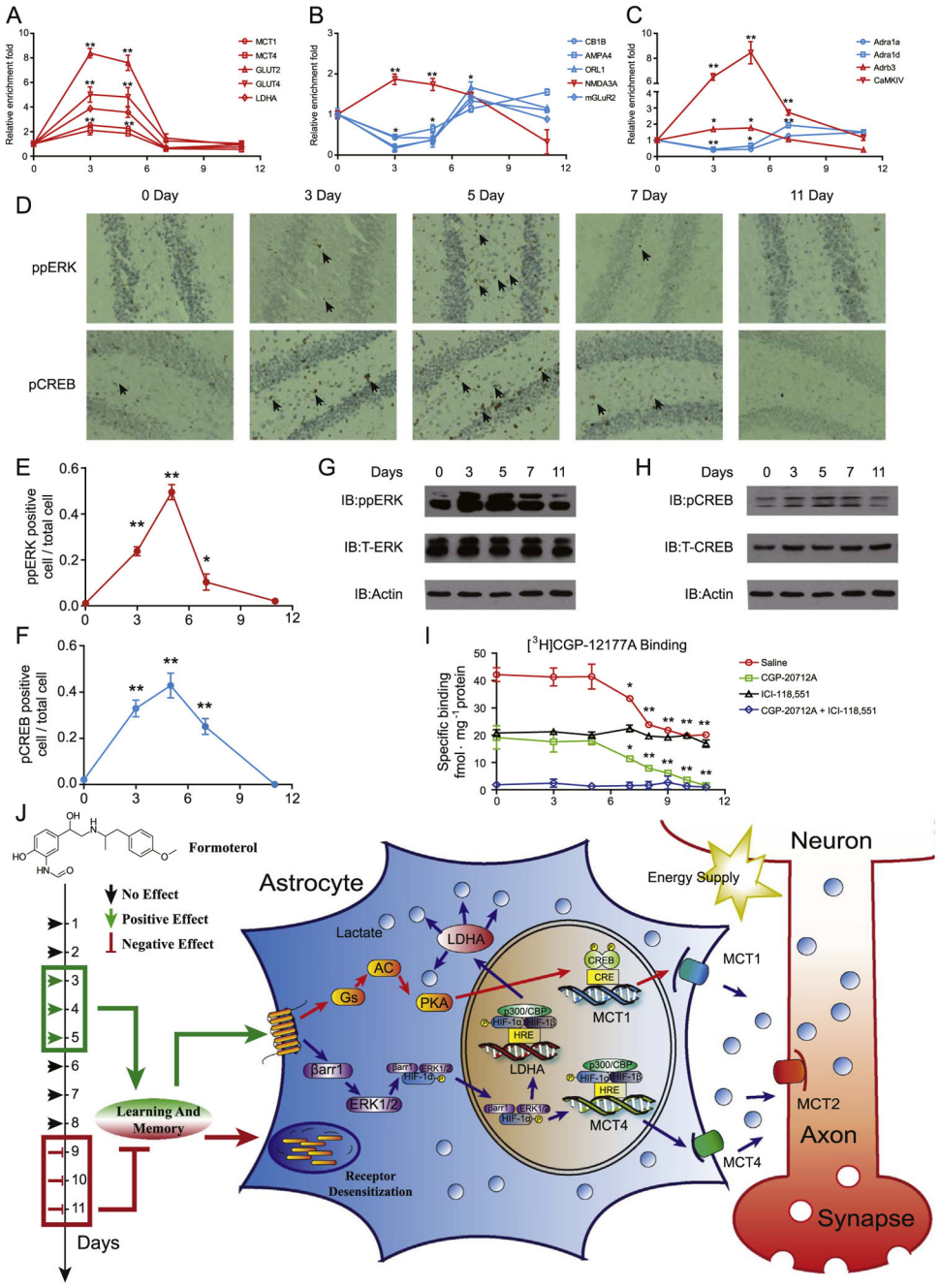

Figure 8.

Prolonged activation of β_2-adrenergic receptor (β2AR) causes desensitization. **(A–C)** Quantitative reverse transcriptase polymerase chain reaction analysis of messenger RNA levels of genes important for β2AR-dependent signaling networks after formoterol stimulation for 3, 5, 7, or 11 days. Genes enriched in **(A)** the lactate metabolism and transport network, **(B)** the glutamate receptor-synaptic long-term potentiation signaling network, and **(C)** the calcium signaling network. Red, genes that exhibited an increase on days 3 and 5 compared to the initial date; blue, genes that exhibited a decrease on days 3 and 5 compared to the initial date. **(D)** Representative immunohistochemistry image of phospho-

mitogen-activated protein kinase (ppERK) (upper panel) and phospho-cyclic adenosine monophosphate response element binding protein (pCREB) (lower panel) in the hippocampus after formoterol treatment for 3, 5, 7, and 11 days. **(E, F)** Statistical analysis and line chart representing the percentage of cells with positive staining of ppERK or pCREB in **(D)** (six sections were randomly selected from each mouse. $n = 6$ for each group of mice.). **(G, H)** Western blot of ppERK or pCREB in the hippocampus from the wild-type mice treated with formoterol for 3, 5, 7, or 11 days (upper panel). Representative blots from at least three independent experiments are shown. Protein levels of total ERK (T-ERK) and total CREB (T-CREB) were also examined with specific antibodies (middle panel). **(I)** β2AR protein levels in the plasma membrane fraction of the hippocampus from wild-type mice treated with formoterol for 3, 5, 7, or 11 days. Then, 100 nmol/L of [3H]CGP-12177A was used for radioligand binding experiments to measure βAR protein levels on the plasma membrane in the hippocampus. Next, 10 μmol/L of CGP-20712A (specific β1AR antagonist) or 10 μmol/L of ICI 118,551 (specific β2AR antagonist) was used to block specific β1AR or β2AR binding, respectively (saline: * $p = .0288$; ** $p = .0098$, $p = .0089$, $p = .0080$, $p = .0074$; CGP-20712A: * $p = .0350$; ** $p = .0099$, $p = .0081$, $p = .0076$, $p = .0052$). **(J)** Administering a suitable dose of the clinical drug formoterol improves learning and memory in treatment lasting a few days (3–5 days), whereas administration times longer than 1 week are harmful (9–11 days). The beneficial effect of formoterol occurs through β2AR activation. Transcriptional profile analysis and cellular studies revealed that β2AR activation promoted lactate metabolism through both the Gs-protein kinase A (PKA)-CREB-MCT1 and β-arrestin-1-ERK-HIF-1α-MCT4/LDHA pathways. The lactate-shuttling cycle between astrocytes and neurons is required for improved cognitive function stimulated by formoterol treatment in the early days. In contrast, prolonged formoterol administration caused desensitization of β2AR and decreased cognitive ability. **(A–I)** * $p < .05$; ** $p < .01$; formoterol-treated samples were compared with nontreated (0 day) samples. Adra1a, adrenergic receptor, alpha 1a; Adra1d, adrenergic receptor, alpha 1d; Adrb3, adrenergic receptor, beta 3; AMPA4, glutamate receptor, ionotropic, alpha-amino-3-hydroxy-5-methyl-4-isoxazolpropionate receptor 4; CaMKIV, calcium/calmodulin-dependent protein kinase IV; CB1B, cannabinoid receptor 1; GLUT2, glucose transporter 2; IB, immunoblot; LDHA, lactate dehydrogenase A; MCT1, monocarboxylate transporter 1; mGLuR2, metabotropic glutamate receptor 2 (G-protein-coupled receptor type); NMDA3A, *N*-methyl-D-aspartate receptor 3A (glutamate receptor, ion channel type); ORL1, opioid receptor-like 1.